

1 Manuscript submitted as Research Report to *Marine Pollution Bulletin*

2 **Combined effects of fishing and oil spills on marine fish: role of stock**  
3 **demographic structure for offspring overlap with oil**

4 Running head: Demography and oil spill effects

5 Leif Chr. Stige<sup>1,\*</sup>, Geir Ottersen<sup>1,2</sup>, Natalia A. Yaragina<sup>3</sup>, Frode B. Vikebø<sup>2</sup>, Nils Chr.

6 Stenseth<sup>1,4</sup>, Øystein Langangen<sup>1</sup>

7 <sup>1</sup>Centre for Ecological and Evolutionary Synthesis (CEES), Department of Biosciences,  
8 University of Oslo, P.O. Box 1066 Blindern, N-0316 Oslo, Norway.

9 <sup>2</sup>Institute of Marine Research, P.O. Box 1870, N-5817 Bergen, Norway

10 <sup>3</sup>Polar Research Institute of Marine Fisheries and Oceanography (PINRO), 6 Knipovich  
11 Street, Murmansk 183038, Russia.

12 <sup>4</sup>The Centre for Coastal Research, University of Agder, P.O. Box 422, N-4604  
13 Kristiansand, Norway.

14 \*Corresponding author: tel: +47 22854608; fax: +47 22854001; e-mail:

15 *l.c.stige@ibv.uio.no*

16

17 **Abstract**

18 It has been proposed that the multiple pressures of fishing and petroleum activities  
19 impact fish stocks in synergy, as fishing-induced demographic changes in a stock may  
20 lead to increased sensitivity to detrimental effects of acute oil spills. High fishing  
21 pressure may erode the demographic structure of fish stocks, lead to less diverse  
22 spawning strategies, and more concentrated distributions of offspring in space and  
23 time. Hence an oil spill may potentially hit a larger fraction of a year-class of offspring.  
24 Such a link between demographic structure and egg distribution was recently  
25 demonstrated for the Northeast Arctic stock of Atlantic cod for years 1959–1993. We  
26 here estimate that this variation translates into a two-fold variation in the maximal  
27 proportion of cod eggs potentially exposed to a large oil spill. With this information it is  
28 possible to quantitatively account for demographic structure in prospective studies of  
29 population effects of possible oil spills.

30 **Key words:** oil spill; fishing; multiple stressors; fish eggs; Atlantic cod *Gadus morhua*;  
31 Barents Sea

32 **Highlights**

- 33 • We quantify maximal potential overlap between fish eggs and hypothetical oil  
34 spills
- 35 • Maximal overlap is highest when the spawning stock is dominated by small fish
- 36 • Fishing may thus influence sensitivity to oil spills through effect on demography
- 37 • Our results can be used in prospective studies to correct for this effect

## 38 **Introduction**

39 Multiple stressors such as over-exploitation and pollution often impact natural systems  
40 non-additively, implying a need to study such impacts in concert (Crain et al., 2008).  
41 High fishing pressure has led to demographic changes in many fish stocks, towards  
42 increased dominance of young and small spawners (Law, 2000; Longhurst, 2002;  
43 Berkeley et al., 2004; Ottersen, 2008). It is feared that heavy fishing thereby increases  
44 the stocks' sensitivity to environmental influences, including effects of acute oil spills  
45 (Hjermann et al., 2007). Specifically, erosion of demographic structure may reduce the  
46 diversity of spawning strategies and the spatiotemporal distribution of eggs and larvae  
47 (Kjesbu et al., 1992; Opdal, 2010; Opdal and Jørgensen, 2015), which are life-stages  
48 thought to be particularly sensitive to toxic oil compounds (e.g., Carls et al., 1999;  
49 Sørhus et al., 2015). Hence, the proportional overlap between these sensitive early  
50 life-stages and oil in the case of an oil spill may increase. However, quantitative  
51 knowledge on how erosion of spawning stock structure influences potential overlap of  
52 offspring with oil is scarce.

53         The Northeast Arctic (NEA) stock of Atlantic cod *Gadus morhua* is currently the  
54 world's largest and of high economic and ecological importance (Kjesbu et al., 2014).  
55 Spawning occurs along the west and north coasts of Norway from mid-February to  
56 early May (Ottersen et al., 2014) and the eggs and larvae drift pelagically north- and  
57 eastwards towards the Barents Sea nursery area (Olsen et al., 2010). The drift path of  
58 the eggs and larvae crosses areas with ongoing oil activities as well as areas that are  
59 closed for such activities due to concern for fisheries and the environment – a topic of  
60 political and scientific debate (Misund and Olsen, 2013; Blanchard et al., 2014).

61 Statistical analyses of egg survey data for NEA cod for 1959–1993 revealed  
62 positive associations of distributional extent of cod eggs with mean weight (and  
63 alternatively, age) in the spawning stock, spawning stock biomass and a liver condition  
64 index (Stige et al., 2017). We here build on results of Stige et al. (2017) and use the  
65 same egg survey data to quantify in more detail how changes in mean weight and  
66 biomass of spawners are likely to influence the egg distribution and thereby the  
67 potential overlap between eggs and oil. We first consider a case study where overlap  
68 between oil and cod eggs is simulated for a large oil spill near the main spawning  
69 grounds of NEA cod for one year, and assess how hypothetical changes in egg  
70 distribution associated with demographic variables influences overlap calculations.  
71 Subsequently, we construct an index of “worst-case” overlap rate by identifying the  
72 areas with highest cod egg concentrations and calculating how large a fraction of a  
73 year-class is maximally contained within an area of a given size. We then assess how  
74 this fraction depends on spawning stock biomass and mean weight of spawners. We  
75 thus quantify the roles of stock size and demographic structure in influencing potential  
76 year-class susceptibility to geographically bounded events such as oil spills. We  
77 hypothesize that both low mean weight and low total biomass of spawners lead to  
78 increased susceptibility to oil spills.

## 79 **Methods**

### 80 **Data**

81 Eggs of NEA cod were sampled during dedicated ichthyoplankton surveys by the Polar  
82 Research Institute of Marine Fisheries and Oceanography (PINRO), Murmansk  
83 (Mukhina et al., 2003). The survey covered main drift areas of eggs and larvae of NEA  
84 cod between 67°30'N and 74°30'N from about 7 km (4 nautical miles) to 500 km from

85 the coast. From around 10 % to 25 % of the landings from the fisheries on spawning  
 86 fish in years 1959–1969 were from south of the survey area (Opdal, 2010), with the  
 87 long-term trends in the proportion apparently covarying with the mean age of the  
 88 spawners [(Opdal and Jørgensen, 2015) but see (Sundby, 2015)]. The survey was  
 89 conducted in April–May, i.e. 0–2 months after the peak spawning of the cod (Ellertsen  
 90 et al., 1989), each year from 1959 to 1993, except 1967, when there was no survey. On  
 91 average 156 stations were sampled each year, but with considerable variability among  
 92 years in the extent and timing of the survey (Mukhina et al., 2003; Stige et al., 2015).  
 93 Cod eggs were classified into four developmental stages based on morphology. Stage-1  
 94 eggs could not be reliably differentiated from the eggs of haddock. Stage-1 eggs were  
 95 therefore classified to species according to the fraction of cod compared to haddock  
 96 eggs of stages 2–4 in the sample. For further details on the ichthyoplankton data we  
 97 refer the reader to Mukhina et al. (2003) and Stige et al. (2015).

98 Spawning stock biomass (*SSB*, tonnes) data were obtained from ICES (2009).  
 99 *SSB* is computed using values for stock number at age from extended survivors analysis  
 100 (*XSA*) based mainly on fisheries data, weight-at-age in the stock and maturity-at-age,  
 101 calculated as weighted averages from Russian and Norwegian surveys during the  
 102 autumn and winter seasons (Marshall et al., 2006; ICES, 2009). We used log-  
 103 transformed biomass,  $\log SSB = \log_e(SSB)$ , hence assuming a log-linear relationship with  
 104 egg abundance in the statistical analysis.

105 Mean biomass-weighted weight in the spawning stock ( $\bar{W}$ , kg) was calculated  
 106 from abundance-at-age estimated by *XSA*, weight-at-age and maturity-at-age, all from  
 107 ICES (2009):

108 (1) 
$$\bar{W}_j = \frac{\sum_{a=3}^{a=13+} W_{aj}(N_{aj}W_{aj}M_{aj})}{\sum_{a=3}^{a=13+} (N_{aj}W_{aj}M_{aj})}$$

109 Here,  $N_{aj}$ ,  $W_{aj}$  and  $M_{aj}$  are, respectively, number, mean weight (kg) and proportion  
110 mature at age  $a$  in year  $j$ . The product ( $N_{aj}W_{aj}M_{aj}$ ) is thus mature biomass-at-age and  
111 the denominator sums up to  $SSB_j$ . By weighting by biomass and not abundance of  
112 each age class,  $\bar{W}$  represents the sizes that dominate the spawning stock in terms of  
113 potential egg production.  $\bar{W}$  is highly correlated with mean age in the spawning stock  
114 (product-moment correlation,  $r = 0.92$ ).

115 The liver condition index ( $COND$ , %) is liver wet weight, measured as  
116 percentage of total wet weight for cod of lengths 41–70 cm for January–December the  
117 year before spawning (Yaragina and Marshall, 2000).

#### 118 **Statistical analysis of how spawning stock variables influence egg distribution**

119 To quantify the change in spatial distribution of cod eggs under contrasting biomass  
120 and size structure in the spawning stock, we fit a spatiotemporal statistical model to  
121 the cod egg data. Following results of time-series analyses by Stige et al. (2017)  
122 identifying significant predictors of cod egg distributional extent, we included sampling  
123 day-of-year ( $Day$ ), sampling location ( $Lon$ , °N, and  $Lat$ , °E),  $COND$ ,  $\bar{W}$  and  $logSSB$  as  
124 predictor variables. Following the same results, no abiotic environmental variables  
125 were included. The spatiotemporal statistical model was used to estimate the spatial  
126 distribution of cod eggs as function of  $\bar{W}$  and  $logSSB$  and mean values of the other  
127 predictor variables. Specifically, the expected stage-specific and total egg abundances  
128 at different locations in the survey area at a date representing a peak in observed egg  
129 abundance halfway through their development (10<sup>th</sup> April) were calculated by  
130 multiplying estimated probabilities from a binomial submodel with estimated  
131 conditional abundances from a lognormal submodel. The spatiotemporal statistical  
132 model is described in detail in the Appendix.

### 133 **Simulation of overlap between oil and fish offspring**

134 To illustrate how spawning stock size and demographic structure can be accounted for  
135 in oil spill simulations we used results from Vikebø et al. (2014), who modelled overlap  
136 between oil compounds and eggs and larvae of NEA cod for four hypothetical oil spill  
137 scenarios, all simulated for the same year (i.e., 1997). The modelling is described in  
138 details by Vikebø et al. (2014) and only summarised here. Specifically, 94 500 particles  
139 each representing a large number of cod eggs were released at the known spawning  
140 grounds and in the spawning period (1 March – 30 April) of NEA cod and transported  
141 horizontally based on their vertical positioning in the water column and ocean currents.  
142 Ocean currents were simulated using a regional ocean model system for the Nordic  
143 Seas with resolution 4×4 km (Lien et al., 2014). The transport and fate of oil  
144 compounds were simulated based on the same ocean model. We here investigated  
145 two oil spill scenarios representing a large oil spill at the peak of the spawning season  
146 (i.e., 4500 tonnes of oil per day for 30 days, 1–30 April) but differing in oil spill location  
147 (scenario 1: N 68.67, E 13.92, scenario 2: N 68.83, E 13.45). Two other scenarios with  
148 oil spill locations farther south investigated by Vikebø et al. (2014) were not analysed  
149 here because the majority of the impacted eggs were outside of the survey area (N  
150 67.5–74.5, E 8–31.5). For each particle we found the maximal concentration of total  
151 polycyclic aromatic hydrocarbon (TPAH) along its drift trajectory through the egg and  
152 larval stages, here using the highest concentration in the water column (Vikebø et al.,  
153 2014, also considered ambient concentrations at the depths of the particles). Overlap  
154 was calculated as percentage of individuals having maximal TPAH concentration above  
155 thresholds of 0.1 parts per billion (ppb) or 1.0 ppb, representing, respectively, order of  
156 magnitude thresholds for sublethal and lethal effects. Note that work is still ongoing to  
157 refine these values for different stages and species.

158           The simulation results of Vikebø et al. (2014) represent a historical average  
159 situation in terms of spawning stock size and –structure. To assess the effect of  
160 altering  $\bar{W}$  or  $\log SSB$  we weighted the particles, i.e. the number of individuals each  
161 particle represented, based on the results of the statistical analysis of how spawning  
162 stock variables influence egg distribution. The weighting was based on the location of  
163 the particles half-way through the egg development, i.e., around the transition from  
164 the second to the third egg stage. To simulate the egg distribution expected under high  
165  $\bar{W}$  each particle was weighted by the predicted egg abundance for that location for the  
166 90<sup>th</sup> percentile of  $\bar{W}$  divided on the prediction for the same location for mean  $\bar{W}$ . The  
167 predictions were for total numbers of stage-2 and stage-3 eggs at April 10, which was  
168 between the peaks of abundance for these two stages. Note that effects of  $\bar{W}$  and  
169  $\log SSB$  on egg distribution in the statistical model were assumed to be independent of  
170 day-of-year and egg stage (at the linear scales of the predictors in the binomial and  
171 lognormal submodels); hence the application of these weights based on locations at a  
172 single developmental stage independent of when that stage is reached is consistent  
173 with the statistical model. Particles outside of the survey area (representing 20 % of  
174 the individuals) were excluded from the analysis in order to avoid extrapolation.  
175 Subsequently we calculated the fraction of the year-class exposed to sublethal or  
176 lethal concentrations of oil for each oil spill scenario. Corresponding calculations were  
177 made for the 10<sup>th</sup> percentile of  $\bar{W}$  and for the 10<sup>th</sup> and 90<sup>th</sup> percentile of  $\log SSB$ .

178   **How does “worst-case” potential overlap rate depend on spawning stock variables?**

179 While the oil spill simulation illustrates the role of stock size and demographic  
180 structure for two oil spill scenarios, other scenarios with the same spatial extent but  
181 different locations of oil could conceivably give higher overlap with cod eggs and larvae



182 (e.g., Carroll et al., 2018). We thus constructed an index of maximum number of cod  
183 eggs contained within an area representative of a large oil spill and investigated how  
184 this index varied with spawning stock variables. To construct this index we used the  
185 spatiotemporal statistical model of how spawning stock variables influence egg  
186 distribution and calculated stage-specific as well as total egg abundance for a grid at  
187 fixed 1° longitude and 1/3 ° latitude intervals over the study area. The area  
188 represented by each grid cell is given by  $Area_i = 20 \cdot 1.852 \cdot 60 \cdot 1.852 \cdot \cos(\pi \cdot Lat_i / 180)$   
189  $km^2$  and varied from 1111  $km^2$  in the north to 1564  $km^2$  in the south. For given values  
190 of  $\bar{W}$  and  $logSSB$  we ranked the grid cells according to expected egg concentration and  
191 calculated the cumulative number of expected eggs as function of cumulative area.  
192 Note that these grid cells were not necessarily contiguous. We then compared the  
193 maximal proportions of the eggs contained within 10 000  $km^2$  or 40 000  $km^2$   
194 dependent on  $\bar{W}$  and  $logSSB$ . These area sizes represent the approximate range in  
195 surface coverage of oil components at lethal concentrations in a large oil spill scenario  
196 for the region (Vikebø et al., 2014; Langangen et al., 2017).

197 In the presence of strong compensatory density dependence locally (e.g.,  
198 Ciannelli et al., 2007), distribution area may hypothetically be a better proxy for year-  
199 class strength than abundance. We therefore also calculated maximal proportion of  
200 the total cod egg distribution area ( $km^2$ ) contained within 10 000  $km^2$  or 40 000  $km^2$ .  
201 For this calculation, egg occupancy area was calculated for each grid cell by multiplying  
202 grid cell area with expected probability of cod egg occurrence dependent on  $\bar{W}$  and  
203  $logSSB$ .

204 The uncertainty of the estimates was quantified by non-parametric bootstrap,  
205 whereby we generated 1000 bootstrap data sets by resampling years (with

206 replacement) and analysed the bootstrap data sets with the same procedure as the  
207 original data.

208 The analyses were performed using the programming environment R version  
209 3.2.4 (R Core Team, 2016). The mgcv package version 1.8-12 (Wood, 2006) in R was  
210 used for generalized additive modelling.

## 211 Results

212 The size and demographic structure of the spawning stock of NEA cod varied  
213 considerably during the studied period 1959–1993 (**Fig. S1**), with *SSB* varying by a  
214 factor of 9 between 0.10 million tonnes ( $\log SSB = 11.5$ , in 1965) and 0.89 million  
215 tonnes ( $\log SSB = 13.7$ , in 1992), and  $\bar{W}$  varying between 2.8 kg (in 1990) and 7.9 kg (in  
216 1974). The variation in  $\log SSB$  and  $\bar{W}$  was uncorrelated (product-moment correlation  $r$   
217 = -0.04), allowing us to study each factor independently.

218 The generalized additive model results showed a wider spatial distribution of  
219 cod eggs at high compared to low  $\bar{W}$  and at high compared to low  $\log SSB$  (**Fig. 1**). We  
220 find that at high  $\log SSB$ , cod egg concentrations were particularly high off the main  
221 spawning grounds at 68–70 °N, while there was no such peak at low  $\log SSB$  (**Fig. 1**).

222 Results of the oil spill simulation showed that adjusting the egg distribution to  
223 that expected at low or high  $\bar{W}$  or low or high  $\log SSB$  changed the calculated oil spill  
224 effects by approximately  $\pm 5\%$  for the scenarios considered (see **Table 1** for exact  
225 numbers and **Fig. S2** for spatial distributions of eggs with drift paths overlapping or not  
226 with above-threshold concentrations of oil).

227 The maximal proportion of cod eggs contained within areas of 10 000 km<sup>2</sup> or  
228 40 000 km<sup>2</sup> was about two times higher at the low end of the  $\bar{W}$  range compared to at

229 the high end of the  $\bar{W}$  range (**Fig. 2A**). Specifically, the maximal proportion of cod eggs  
230 contained within an area of 40 000 km<sup>2</sup> was 0.32 (95 % confidence intervals, c.i.: 0.24,  
231 0.40) at  $\bar{W} = 7.9$  kg and 0.57 (c.i.: 0.42, 0.71) at  $\bar{W} = 2.8$  kg. The corresponding  
232 proportions for 10 000 km<sup>2</sup> were 0.13 (c.i.: 0.07, 0.21) at high  $\bar{W}$  and 0.29 (c.i.: 0.16,  
233 0.43) at low  $\bar{W}$ . Similarly, the maximal proportion of the total distribution area  
234 contained within areas of 10 000 km<sup>2</sup> or 40 000 km<sup>2</sup> were higher at low compared to  
235 high  $\bar{W}$  (**Fig. S3**).

236 Contrary to hypothesized, the maximal proportion of cod eggs contained within  
237 areas of 10 000 km<sup>2</sup> or 40 000 km<sup>2</sup> were higher at high compared to low *logSSB* (**Fig.**  
238 **2B**). This result is linked to the high concentrations of cod eggs found near the main  
239 spawning grounds at high *logSSB* (**Fig. 1**). According to our estimates, nearly 80 % of  
240 the cod eggs can be contained within an area of 40 000 km<sup>2</sup> in years with high *logSSB*,  
241 compared with maximally around 40 % in years with low *logSSB*. On the other hand,  
242 the maximal proportion of the total distribution area contained within areas of 10 000  
243 km<sup>2</sup> or 40 000 km<sup>2</sup> were higher at low compared to high *logSSB* (**Fig. S3**), which is a  
244 direct result of the total distribution area being smallest at low *logSSB*. Results for  
245 single egg stages (**Fig. S4**) resembled those for total egg abundance (**Fig. 2**).

## 246 Discussion

247 Our results show that fishing, by influencing size and demographic structure of the  
248 spawning stock (Law, 2000; Longhurst, 2002; Berkeley et al., 2004), may affect the  
249 potential overlap between offspring and oil in the case of an oil spill. Such an influence  
250 of the multiple pressures of fishing and oil has been suggested before (Hjermann et al.,  
251 2007; Rooker et al., 2013), but the quantitative value and hence the potential  
252 importance has until now been generally unknown.

253           The oil spill simulation illustrates how potential changes in egg distribution  
254 caused by changes in stock size and demographic structure can be accounted for in  
255 prospective studies. In these particular scenarios the effects of changes in spawning  
256 stock variables on overlap between oil and fish offspring were found to be small. The  
257 similarity in results for the scenarios considered is probably related to the alternative  
258 oil spill locations being relatively close to one another and that only one year was  
259 considered. It should be noted that there appeared to be fewer simulated egg particles  
260 in offshore regions than expected from the observation data (**Fig. S2** cf. **Fig. 1**) and lack  
261 of particles in these marginal areas could lead to underestimation of the effect of  $\bar{W}$   
262 on variability in egg distribution and hence overlap rate. Moreover, we found that that  
263 worst-case overlap rate is more strongly dependent on stock size and demographic  
264 structure than what overlap rate is for these scenarios.

265           Demographic structure has the clearest effect, and we find that potential  
266 overlap rate, measured as maximal proportion of eggs contained within an area of size  
267 as a large oil spill, varies by a factor of two in response to the near three-fold variation  
268 in  $\bar{W}$  observed for NEA cod in the 1959–1993 period. Potential overlap rate is highest  
269 when  $\bar{W}$  is low, as the eggs are then concentrated in a smaller area than when  $\bar{W}$  is  
270 high. Low  $\bar{W}$  signifies a low proportion of old and large fish in the spawning stock, a  
271 commonly described consequence of high and often size-selective fishing pressure  
272 (Law, 2000; Longhurst, 2002; Ottersen, 2008). A high proportion of old and large  
273 spawners may lead to wide offspring distribution, by allowing for a high diversity in  
274 spawning strategies (e.g., location and duration of spawning) and offspring traits (e.g.,  
275 viability and egg buoyancy) that influence offspring distribution (as discussed by Hixon  
276 et al., 2014; Stige et al., 2017). Note that our analysis mainly quantified effects of  $\bar{W}$  on  
277 spatial distribution; a possible seasonal contraction of spawning at low  $\bar{W}$  (Wright and

278 Trippel, 2009) would tend to accentuate the negative effect of  $\bar{W}$  on potential overlap  
279 rate.

280 Spawning stock biomass has a less clear effect: An oil spill may potentially hit a  
281 larger fraction of the eggs but a smaller fraction of the egg distribution area when  
282  $\logSSB$  is high. This is because at high  $\logSSB$ , there is a peak in egg abundance off the  
283 main spawning grounds, at the same time as the margins of the egg distribution area  
284 expand. The mechanisms behind this peak in egg abundance at high  $\logSSB$  are not  
285 clear. The magnitude of  $\logSSB$  effects on potential overlap rate is similar to that of  $\bar{W}$ .

286 The population consequences of an oil spill hitting eggs in parts of the  
287 distribution depend on the spatial pattern in natural mortality (Langangen et al., 2017).  
288 Natural mortality in central parts of the distribution appears to be higher than in  
289 marginal areas (Ciannelli et al., 2007; Langangen et al., 2014a); hence, a high fraction  
290 of eggs killed if an oil spill hits these areas does not necessarily translate into high  
291 cohort loss in the long-term. This is because eggs in the high-density area have very  
292 low survival anyway. For  $\bar{W}$  we get similar results if potential overlap rate is calculated  
293 from total egg abundance or from distribution area, suggesting that results also hold if  
294 local-scale compensatory density dependence in survival is strong. For  $\logSSB$  on the  
295 other hand, the direction of its effect on maximal long-term impact of an oil spill  
296 depends on how survival is regulated locally.

297 Prospective simulation studies of potential overlap between oil spills and early  
298 life stages of fish (e.g., Vikebø et al., 2014; Carroll et al., 2018) typically, due to lack of  
299 information, ignore effects of spawning stock size and demographic structure on  
300 offspring distribution and exposure. We propose that future studies on NEA cod may  
301 assess effects of possible changes in spawning stock size or demographic structure as

302 implemented in our oil spill simulation. Future studies on other stocks that lack long-  
303 term egg distribution data may use results in **Fig. 2** to assess how large uncertainty is  
304 introduced by ignoring these effects, e.g., quantitatively formalized in a Bayesian  
305 Network model (cf. Carroll and Smit, 2011) or as a correction factor. For example, if a  
306 study finds a maximal impact of 43 % (Carroll et al., 2018) of a year class assuming  
307 average values for  $\bar{W}$ , we suggest that one can conservatively correct this value based  
308 on the results presented here. Based on Fig. 2A, we suggest that adding 0.5 on logit  
309 scale would correct for potential increase in impact caused by reduction in  $\bar{W}$  from the  
310 average value to the minimum observed  $\bar{W}$ . Hence, we suggest correcting the assessed  
311 impact from 43 to 55 % (as  $\text{logit}(0.43) + 0.5 = \text{logit}(0.55)$ ) if one wants to account for  
312 the potential increased impact caused by a hypothetical future reduction in  $\bar{W}$ . In  
313 principle, hypothetical future changes in  $\logSSB$  can be accounted for similarly, but  
314 with a less solid theoretical underpinning than for  $\bar{W}$ : Our statistical results suggest  
315 that the highest proportion of a year class of cod eggs can be lost in years with high  
316  $\logSSB$ , but the causal basis for the distribution changes that drive this result is unclear,  
317 as are the implications for long-term cohort loss.

318         While our results provide quantitative estimates, there are some caveats and  
319 limitations. First, we stress that the analysis of potential overlap rate (**Fig. 2**) indicates  
320 how  $\bar{W}$  or  $\logSSB$  affect “worst-case” effects of oil spills. These “worst-case” effects  
321 can be thought of as the upper tails in the probability distribution for overlap rate if an  
322 oil spill of a given size hits a random part of the study area: With low  $\bar{W}$  this tail is  
323 longer. The analysis therefore does not necessarily reflect how the most likely effect of  
324 a given oil-spill scenario varies with  $\bar{W}$  or  $\logSSB$ , as indeed illustrated by the oil spill  
325 simulation.

326 Further, our calculated potential overlap rate should be interpreted as an index  
327 and not as an accurate estimate of maximal overlap between fish offspring and oil for  
328 a given oil spill size; for such estimates simulation modelling is needed for obtaining  
329 more realistic distributions of oil and appropriately accounting for temporal aspects  
330 and small-scale patchiness. To throw more light on the temporal aspect we assessed  
331 the spatial distribution of simulated eggs in the oil spill model at a snap-shot in time,  
332 finding that eggs having above-threshold oil concentrations at some point in their egg  
333 and larval drift trajectory were concentrated in areas of similar size as used in our  
334 calculation of potential overlap (**Fig. S5**). We therefore consider that our results are  
335 also relevant for oil spills occurring near the drift paths of eggs and larvae over an  
336 extended period. We find it unlikely that our simplifying assumption that overlap  
337 between fish offspring and oil only depends on the horizontal, and not vertical,  
338 locations of fish offspring and oil interferes with our conclusions regarding effects of  $\bar{W}$   
339 or  $\log SSB$  on overlap rate. As shown by Vikebø et al. (2014, their Table 5), relaxing this  
340 assumption will, in general, reduce the overlap rate by roughly a third, independent of  
341 the area affected by oil. In sum, we therefore believe that our estimates are a good  
342 approximation, with a clear empirical basis, of how the mean weight of the spawners  
343 and spawning stock biomass may influence maximal contact rate between fish  
344 offspring and oil.

345 We conclude that loss of old and large fish from a stock due to high fishing  
346 pressure may increase its sensitivity to oil spills. Such a synergistic effect of fishing and  
347 oil is both mediated by the potential overlap between offspring and oil (this study) and  
348 by age-truncated fish stocks having reduced demographic buffering against  
349 recruitment failure (Rouyer et al., 2011; Ohlberger and Langangen, 2015). This  
350 conclusion underlines the multiple benefits of good fisheries management, which has

351 contributed to that the biomass of NEA cod now is high and the proportion of old and  
352 large fish appears to be on the increase (Kjesbu et al., 2014).

### 353 ***Supplementary Material***

354 The following figures are available as supplementary online material:

355 **Figure S1.** Spawning stock biomass (*logSSB*) and mean weight in the spawning stock  
356 ( $\bar{W}$ ) of NEA cod from 1959 to 1993.

357 **Figure S2.** Simulated distribution of NEA cod eggs at their locations halfway through  
358 the egg development, showing which eggs experience sublethal or lethal oil  
359 concentrations for two different oil spill scenarios.

360 **Figure S3.** Maximal proportion of the total distribution area of NEA cod eggs contained  
361 within areas of 10 000 km<sup>2</sup> or 40 000 km<sup>2</sup> dependent on  $\bar{W}$  or *logSSB*.

362 **Figure S4.** Maximal proportion of NEA cod eggs contained within areas of 10 000 km<sup>2</sup>  
363 or 40 000 km<sup>2</sup> dependent on  $\bar{W}$  or *logSSB*, shown for each egg developmental stage.

364 **Figure S5.** Simulated distribution of NEA cod eggs at a snap-shot in time (April 10,  
365 1997), showing which eggs experience sublethal or lethal oil concentrations at some  
366 part of their egg and larval drift trajectories for two different oil spill scenarios.

367

### 368 ***Acknowledgements***

369 We thank the Research Council of Norway for support through the project OILCOM  
370 (255487/E40) and Nordforsk through the project "Green Growth Based on Marine  
371 Resources: Ecological and Socio-Economic Constraints" (GreenMAR).

372



## 373 **References**

- 374 Berkeley, S.A., Hixon, M.A., Larson, R., Love, M.S., 2004. Fisheries sustainability via  
375 protection of age structure and spatial distribution of fish populations. *Fisheries*  
376 29, 23-32.
- 377 Blanchard, A., Hauge, K.H., Andersen, G., Fosså, J.H., Grøsvik, B.E., Handegard, N.O.,  
378 Kaiser, M., Meier, S., Olsen, E., Vikebø, F., 2014. Harmful routines? Uncertainty  
379 in science and conflicting views on routine petroleum operations in Norway.  
380 *Mar. Policy* 43, 313-320.
- 381 Carls, M.G., Rice, S.D., Hose, J.E., 1999. Sensitivity of fish embryos to weathered crude  
382 oil: Part I. Low-level exposure during incubation causes malformations, genetic  
383 damage, and mortality in larval pacific herring (*Clupea pallasii*). *Environ. Toxic.*  
384 *Chem.* 18, 481-493.
- 385 Carroll, J., Smit, M., 2011. An Integrated Modeling Framework For Decision Support In  
386 Ecosystem-Based Management: Case Study Lofoten/Barents Sea. Society of  
387 Petroleum Engineers. doi: 10.2118/140431-MS
- 388 Carroll, J., Vikebø, F., Howell, D., Broch, O.J., Nepstad, R., Augustine, S., Skeie, G.M.,  
389 Bast, R., Juselius, J., 2018. Assessing impacts of simulated oil spills on the  
390 Northeast Arctic cod fishery. *Mar. Poll. Bull.* 126, 63-73.
- 391 Ciannelli, L., Dingsør, G.E., Bogstad, B., Ottersen, G., Chan, K.-S., Gjøsæter, H., Stiansen,  
392 J.E., Stenseth, N.C., 2007. Spatial anatomy of species survival: effects of  
393 predation and climate-driven environmental variability. *Ecology* 88, 635-646.
- 394 Crain, C.M., Kroeker, K., Halpern, B.S., 2008. Interactive and cumulative effects of  
395 multiple human stressors in marine systems. *Ecol. Lett.* 11, 1304-1315.
- 396 Ellertsen, B., Fossum, P., Solemdal, P., Sundby, S., 1989. Relation between temperature  
397 and survival of eggs and first-feeding larvae of northeast Arctic cod (*Gadus*  
398 *morhua* L.). *Rapp. P.-v. Réun. Cons. Int. Explor. Mer* 191, 209-219.
- 399 Hastie, T., Tibshirani, R., 1993. Varying-coefficient models. *J. R. Stat. Soc. B* 55, 757-796.
- 400 Hixon, M.A., Johnson, D.W., Sogard, S.M., 2014. BOFFFFs: on the importance of  
401 conserving old-growth age structure in fishery populations. *ICES J. Mar. Sci.* 71,  
402 2171-2185.

403 Hjermmann, D.Ø., Melsom, A., Dingsør, G.E., Durant, J.M., Eikeset, A.M., Røed, L.P.,  
404 Ottersen, G., Storvik, G., Stenseth, N.C., 2007. Fish and oil in the Lofoten-  
405 Barents Sea system: synoptic review of the effect of oil spills on fish populations.  
406 Mar. Ecol. Prog. Ser. 339, 283-299.

407 ICES, 2009. Report of the Arctic fisheries working group (AFWG), 21 - 27 April 2009,  
408 San-Sebastian, Spain. ICES CM 2009\ACOM:01.

409 Kjesbu, O.S., Bogstad, B., Devine, J.A., Gjørseter, H., Howell, D., Ingvaldsen, R.B., Nash,  
410 R.D.M., Skjæraasen, J.E., 2014. Synergies between climate and management for  
411 Atlantic cod fisheries at high latitudes. Proc. Natl. Acad. Sci. USA 111, 3478-  
412 3483.

413 Kjesbu, O.S., Kryvi, H., Sundby, S., Solemdal, P., 1992. Buoyancy variations in eggs of  
414 Atlantic cod (*Gadus morhua* L.) in relation to chorion thickness and egg size:  
415 theory and observations. J. Fish Biol. 41, 581-599.

416 Langangen, Ø., Olsen, E., Stige, L.C., Ohlberger, J., Yaragina, N.A., Vikebø, F.B., Bogstad,  
417 B., Stenseth, N.C., Hjermmann, D.Ø., 2017. The effects of oil spills on marine fish:  
418 Implications of spatial variation in natural mortality. Mar. Poll. Bull., doi:  
419 10.1016/j.marpolbul.2017.1003.1037.

420 Langangen, Ø., Stige, L.C., Yaragina, N.A., Ottersen, G., Vikebø, F.B., Stenseth, N.C.,  
421 2014a. Spatial variations in mortality in pelagic early life stages of a marine fish  
422 (*Gadus morhua*). Progr. Oceanogr. 127, 96-107.

423 Langangen, Ø., Stige, L.C., Yaragina, N.A., Vikebø, F., Bogstad, B., Gusdal, Y., 2014b. Egg  
424 mortality of Northeast Arctic cod (*Gadus morhua*) and haddock  
425 (*Melanogrammus aeglefinus*). ICES J. Mar. Sci. 71, 1129–1136.

426 Law, R., 2000. Fishing, selection, and phenotypic evolution. ICES J. Mar. Sci. 57, 659-  
427 668.

428 Lien, V.S., Gusdal, Y., Vikebø, F.B., 2014. Along-shelf hydrographic anomalies in the  
429 Nordic Seas (1960–2011): locally generated or advective signals? Ocean Dyn. 64,  
430 1047-1059.

431 Longhurst, A., 2002. Murphy's law revisited: longevity as a factor in recruitment to fish  
432 populations. Fish. Res. 56, 125-131.

433 Marshall, C.T., Needle, C.L., Thorsen, A., Kjesbu, O.S., Yaragina, N.A., 2006. Systematic  
434 bias in estimates of reproductive potential of an Atlantic cod (*Gadus morhua*)  
435 stock: implications for stock-recruit theory and management. *Can. J. Fish. Aquat.*  
436 *Sci.* 63, 980-994.

437 Misund, O.A., Olsen, E., 2013. Lofoten-Vesterålen: for cod and cod fisheries, but not for  
438 oil? *ICES J. Mar. Sci.* 70, 722-725.

439 Mukhina, N.V., Marshall, C.T., Yaragina, N.A., 2003. Tracking the signal in year-class  
440 strength of Northeast Arctic cod through multiple survey estimates of egg,  
441 larval and juvenile abundance. *J. Sea Res.* 50, 57-75.

442 Ohlberger, J., Langangen, Ø., 2015. Population resilience to catastrophic mortality  
443 events during early life stages. *Ecol. Applic.* 25, 1348-1356.

444 Olsen, E., Aanes, S., Mehl, S., Holst, J.C., Aglen, A., Gjørseter, H., 2010. Cod, haddock,  
445 saithe, herring, and capelin in the Barents Sea and adjacent waters: a review of  
446 the biological value of the area. *ICES J. Mar. Sci.* 67, 87-101.

447 Opdal, A.F., 2010. Fisheries change spawning ground distribution of northeast Arctic  
448 cod. *Biol. Lett.* 6, 261-264.

449 Opdal, A.F., Jørgensen, C., 2015. Long-term change in a behavioural trait: truncated  
450 spawning distribution and demography in Northeast Arctic cod. *Global Change*  
451 *Biol.* 21, 1521-1530.

452 Ottersen, G., 2008. Pronounced long-term juvenation in the spawning stock of Arcto-  
453 Norwegian cod (*Gadus morhua*) and possible consequences for recruitment.  
454 *Can. J. Fish. Aquat. Sci.* 65, 523-534.

455 Ottersen, G., Bogstad, B., Yaragina, N.A., Stige, L.C., Vikebø, F.B., Dalpadado, P., 2014.  
456 A review of early life history dynamics of Barents Sea cod (*Gadus morhua*). *ICES*  
457 *J. Mar. Sci.* 71, 2064-2087.

458 R Core Team, 2016. R: A language and environment for statistical computing. R  
459 Foundation for Statistical Computing, Vienna, Austria. URL [https://www.R-](https://www.R-project.org/)  
460 [project.org/](https://www.R-project.org/).

461 Rooker, J.R., Kitchens, L.L., Dance, M.A., Wells, R.J.D., Falterman, B., Cornic, M., 2013.  
462 Spatial, Temporal, and Habitat-Related Variation in Abundance of Pelagic Fishes

463 in the Gulf of Mexico: Potential Implications of the Deepwater Horizon Oil Spill.  
464 PLOS ONE 8, e76080.

465 Rouyer, T.A., Ottersen, G., Durant, J.M., Hidalgo, M., Hjermann, D.Ø., Persson, J., Stige,  
466 L.C., 2011. Shifting dynamic forces in fish stock fluctuations triggered by age  
467 truncation? *Global Change Biol.* 17, 3046-3057.

468 Stefánsson, G., 1996. Analysis of groundfish survey abundance data: combining the  
469 GLM and delta approaches. *ICES J. Mar. Sci.* 53, 577-588.

470 Stige, L.C., Langangen, Ø., Yaragina, N.A., Vikebø, F.B., Bogstad, B., Ottersen, G.,  
471 Stenseth, N.C., Hjermann, D.Ø., 2015. Combined statistical and mechanistic  
472 modelling suggests food and temperature effects on survival of early life stages  
473 of Northeast Arctic cod (*Gadus morhua*). *Progr. Oceanogr.* 134, 138-151.

474 Stige, L.C., Yaragina, N.A., Langangen, Ø., Bogstad, B., Stenseth, N.C., Ottersen, G.,  
475 2017. Effect of a fish stock's demographic structure on offspring survival and  
476 sensitivity to climate. *Proc. Natl. Acad. Sci. USA* 114, 1347-1352.

477 Sundby, S., 2015. Comment to 'Opdal AF, Jørgensen C (2015) Long-term change in a  
478 behavioural trait: truncated spawning distribution and demography in  
479 Northeast Arctic cod. *Global Change Biology*, 21:4, 1521–1530, doi:  
480 10.1111/gcb.12773'. *Global Change Biol.* 21, 2465-2466.

481 Sørhus, E., Edvardsen, R.B., Karlsen, Ø., Nordtug, T., van der Meeren, T., Thorsen, A.,  
482 Harman, C., Jentoft, S., Meier, S., 2015. Unexpected Interaction with Dispersed  
483 Crude Oil Droplets Drives Severe Toxicity in Atlantic Haddock Embryos. *PLOS*  
484 *ONE* 10, e0124376.

485 Vikebø, F.B., Rønningen, P., Lien, V.S., Meier, S., Reed, M., Ådlandsvik, B., Kristiansen,  
486 T., 2014. Spatio-temporal overlap of oil spills and early life stages of fish. *ICES J.*  
487 *Mar. Sci.* 71, 970-981.

488 Wood, S.N., 2006. *Generalized additive models: An introduction with R.* Chapman and  
489 Hall/CRC, Boca Raton, FL.

490 Wright, P.J., Trippel, E., 2009. Fishery-induced demographic changes in the timing of  
491 spawning: consequences for reproductive success. *Fish Fisheries* 10, 283-304.

492 Yaragina, N.A., Marshall, C.T., 2000. Trophic influences on interannual and seasonal  
493 variation in the liver condition index of Northeast Arctic cod (*Gadus morhua*).  
494 ICES J. Mar. Sci. 57, 42-55.

495

496 **Appendix**

497 **Spatiotemporal statistical cod egg distribution model**

498 To quantify the change in spatial distribution of cod eggs under contrasting biomass  
499 and size structure in the spawning stock, we fit a variable-coefficient generalized  
500 additive model (Hastie and Tibshirani, 1993; Wood, 2006) to the spatiotemporal cod  
501 egg data. Following results of time-series analysis by Stige et al. (2017), we included  
502 sampling day-of-year (*Day*), sampling location (*Lon*, °N, and *Lat*, °E), *COND*,  $\bar{W}$  and  
503 *logSSB* as predictor variables. As the survey data contained many stations with no eggs,  
504 the data were considered to originate from two different processes: one process  
505 determining the probability of a positive tow (i.e., non-zero abundance of eggs of a  
506 given stage at a station) and another determining the abundance conditional on a  
507 positive tow (see Langangen et al., 2014b). To account for the two processes we used a  
508 hurdle model approach (Stefánsson, 1996), whereby a binomial model quantified the  
509 probability of a positive tow and a lognormal model quantified abundance in positive  
510 tows.

511 The binomial submodel quantified the probability  $p$  of catching at least one  
512 egg of a given stage at a station. Each data point represents presence (coded as 1) or  
513 absence (coded as 0) of one out of four egg developmental stages at one station in one  
514 year. Each station is thus represented by four data points in the analysis, one for each  
515 egg stage. This submodel can be written as:

516 (2) 
$$\text{logit}(p_{s\ ij}) = \alpha_s + f_s(\text{Day}_i) + g_s(\text{Lon}_i, \text{Lat}_i) + \beta \text{COND}_j +$$
  
517 
$$h(\text{Lon}_i, \text{Lat}_i) \bar{W}_j + l(\text{Lon}_i, \text{Lat}_i) \text{logSSB}_j$$

518 where subscripts  $s$ ,  $i$  and  $j$  represent stage, station and year, respectively.  $\alpha_s$  is a stage-  
519 specific intercept.  $f_s$  and  $g_s$  are stage-specific smooth functions correcting for sampling  
520 date and location ( $g_s$  being a two-dimensional anisotropic smooth modelled as a  
521 tensor-product of two smooth basis functions with maximally 5 knots each). Stage-  
522 specific smooths were modelled by using the flag “by=Stage” when specifying the  
523 smooth.  $\beta$  is the coefficient for the effect of *COND*. The coefficients for the effects of  
524  $\bar{W}$  and  $\logSSB$  were allowed to vary smoothly as functions of location. The smooth  
525 function  $h(Lon, Lat)$  thus gives a location-dependent coefficient that  $\bar{W}$  is multiplied  
526 with and  $l(Lon, Lat)$  the corresponding function for  $\logSSB$ . The number of samples  
527 taken at the station was included as offset. This binomial submodel is similar to a  
528 corresponding model with a spatially-variable  $\bar{W}$  term used by Stige *et al.* (2017, Fig. 3)  
529 to visualize how cod egg distribution varies with  $\bar{W}$ . We here allowed the effects of  
530 both  $\bar{W}$  and  $\logSSB$  to vary spatially in order to focus on two factors directly influenced  
531 by human activities, while the effect of *COND* was spatially invariable in order to limit  
532 the number of parameters in the model.

533 Furthermore, in contrast to Stige *et al.* (2017), we also quantified how cod egg  
534 abundance within the distribution area varies with  $\bar{W}$  and  $\logSSB$ . To do so, we  
535 modelled the natural logarithm of cod egg abundance in positive tows,  $\log_e(N)$ , but  
536 using only non-zero counts and assuming a normal error distribution ( $\varepsilon$ ). This  
537 submodel can be summarized as:

$$\begin{aligned}
 (3) \quad \log_e(N_{sij}) &= \gamma_s + m_s(\text{Day}_i) + n_s(\text{Lon}_i, \text{Lat}_i) + \delta \text{COND}_j + \\
 & p(\text{Lon}_i, \text{Lat}_i) \bar{W}_j + q(\text{Lon}_i, \text{Lat}_i) \logSSB_j + \varepsilon_{sij} \quad \text{for } N_{sij} > 0
 \end{aligned}$$

540 The notation is analogous to Eq. 2. For this analysis, the natural logarithm of  
541 the number of samples taken at the station was offset.

542            This hurdle model was used to map the expected total egg abundance as  
543 function of  $\bar{W}$  and  $\log SSB$ . Specifically, we calculated total egg abundance (sum of all  
544 stages) by multiplying predicted probabilities from Eq. 2 with predicted conditional  
545 abundances from Eq. 3 (taking into account that expected  $N$  from Eq. 3 is the exponent  
546 of the expected  $\log_e(N) + \frac{1}{2}$  variance of  $\log_e(N)$ ).

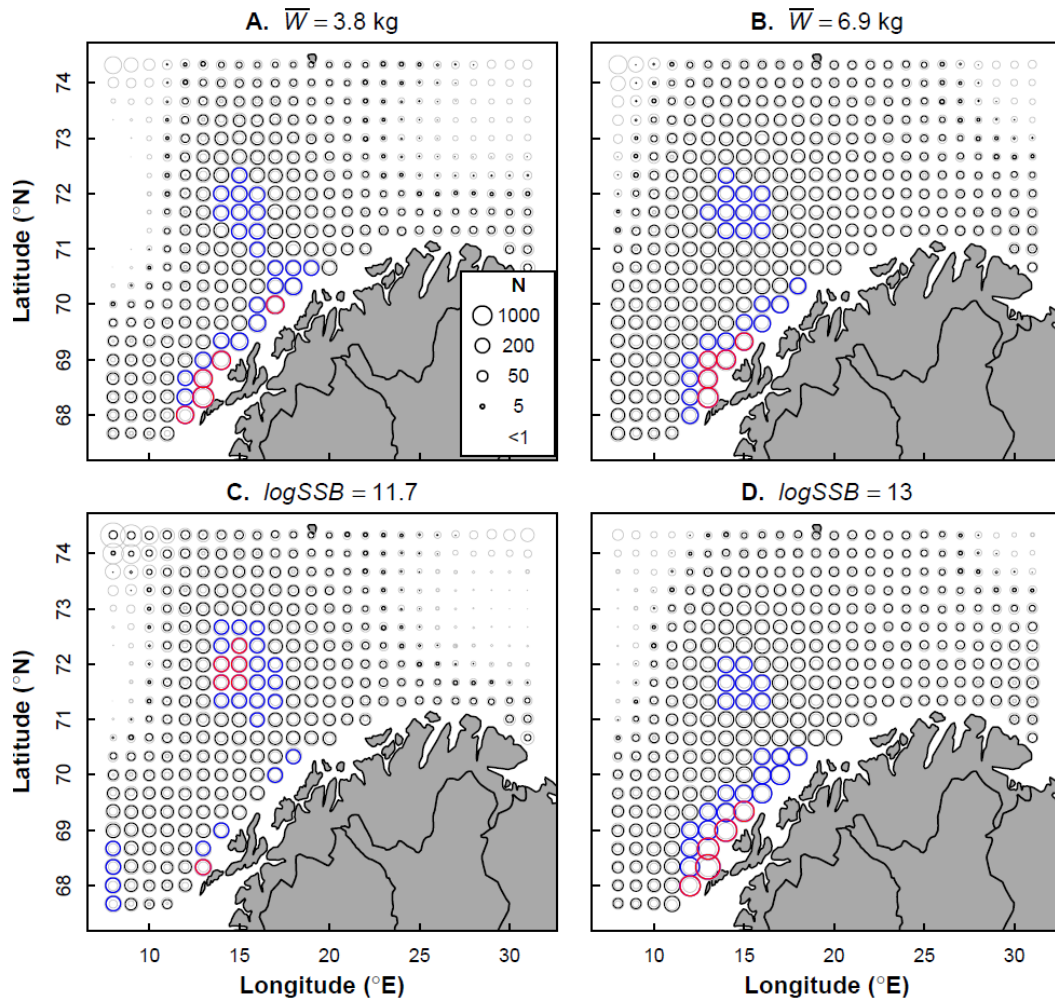


547 **Table 1. Overlap of NEA cod eggs and larvae with oil as function of mean weight in**  
 548 **the spawning stock ( $\bar{W}$ ) and spawning stock biomass ( $logSSB$ ) for two oil spill**  
 549 **scenarios in year 1997 and alternative threshold concentrations of oil compounds.**

550 Percentage overlap [Overlap relative to baseline]

551 Scenario / threshold	Baseline	Low $\bar{W}$	High $\bar{W}$	Low $logSSB$	High $logSSB$
552 Oil spill scenario 1 / 0.1 ppb	20.3 [1]	21.3 [1.05]	19.6 [0.97]	21.0 [1.03]	19.6 [0.97]
553 Oil spill scenario 1 / 1.0 ppb	5.7 [1]	5.9 [1.05]	5.4 [0.96]	5.8 [1.06]	5.5 [0.96]
554 Oil spill scenario 2 / 0.1 ppb	29.8 [1]	31.3 [1.05]	28.6 [0.96]	31.5 [1.02]	28.4 [0.96]
555 Oil spill scenario 2 / 1.0 ppb	11.1 [1]	11.8 [1.06]	10.6 [0.96]	12.0 [1.07]	10.5 [0.95]

556 Baseline:  $\bar{W}$  = 5.5 kg and  $logSSB$  = 12.4, low  $\bar{W}$ : 3.8 kg, high  $\bar{W}$ : 6.9 kg, low  $logSSB$ : 11.7, high  $logSSB$ : 13.0



557

558

559

560

561

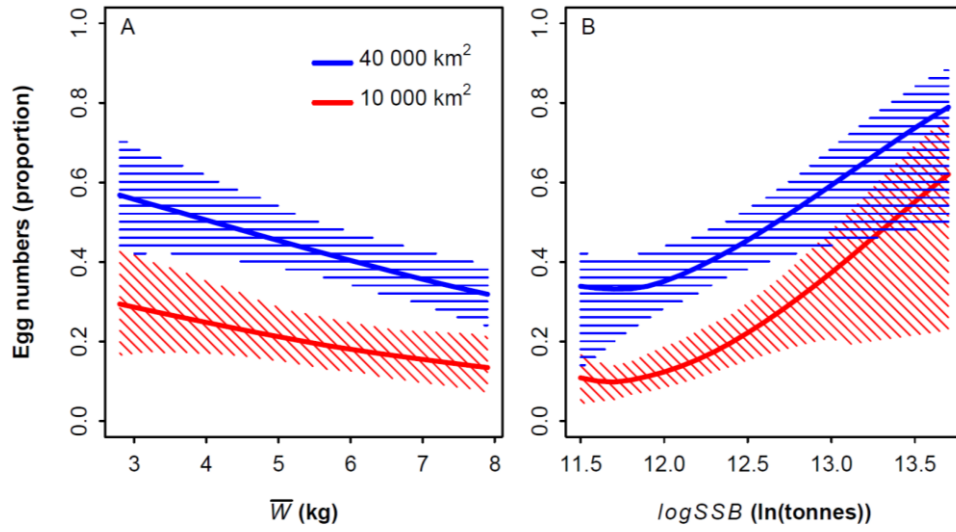
562

563

564

565

**Figure 1.** Expected distribution of Northeast Arctic (NEA) cod eggs at different combinations of mean weight in the spawning stock,  $\bar{W}$ , and spawning stock biomass,  $\logSSB$ . Panels A and B represent 10th and 90th percentile of  $\bar{W}$  and mean  $\logSSB$ . Panels C and D represent 10th and 90th percentile of  $\logSSB$  and mean  $\bar{W}$ . Sizes of circles scale with total expected egg abundance per net haul, with grey circles representing 95 % bootstrap confidence intervals. Red and blue circles show the grid cells representing, respectively, the 10 000 km<sup>2</sup> and 40 000 km<sup>2</sup> with highest egg abundance.



566

567

568

569

570

**Figure 2.** Maximal proportion of NEA cod eggs contained within areas of 10 000 km<sup>2</sup> or 40 000 km<sup>2</sup> dependent on (A) mean weight in the spawning stock,  $\bar{W}$ , or (B) spawning stock biomass,  $\log SSB$ . Hatched lines represent 95 % confidence intervals (horizontal blue lines for 40 000 km<sup>2</sup>, oblique red lines for 10 000 km<sup>2</sup>).

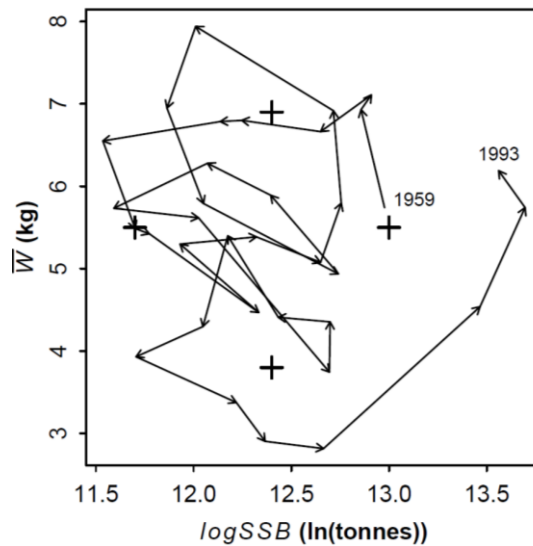
571 **Supplementary Information**

572 This online supplementary information file accompanies the paper:

573 Stige, L.C., Ottersen, G., Yaragina, N.A., Frode B. Vikebø, Stenseth, N.C., and Langangen,  
574 Ø., 2018. Combined effects of fishing and oil spills on marine fish: role of stock  
575 demographic structure for offspring overlap with oil. Marine Pollution Bulletin.

576

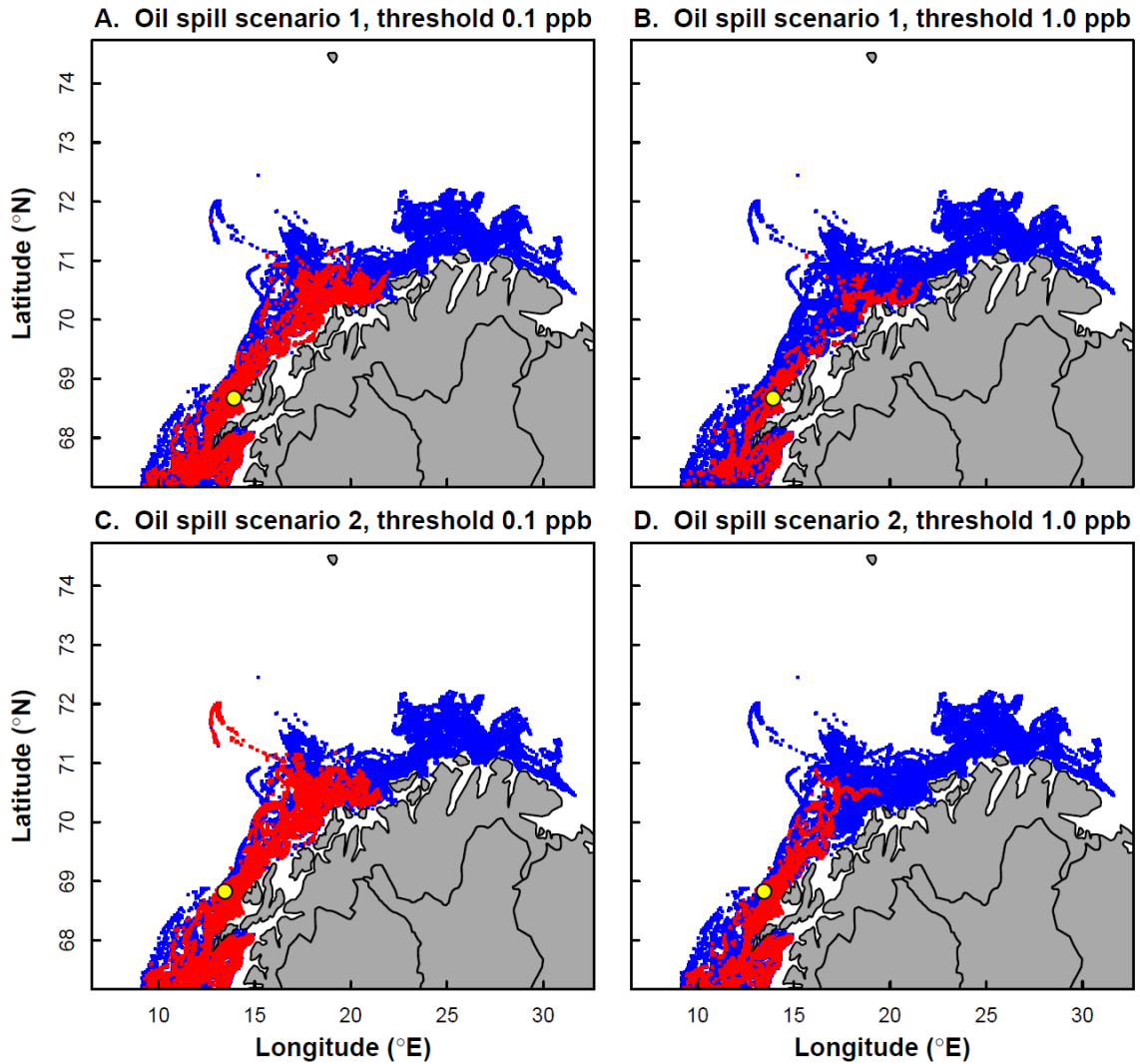
577



578

579 **Figure S1.** Spawning stock biomass ( $\logSSB$ ) and mean weight in the spawning  
580 stock ( $\bar{W}$ ) of Northeast Arctic cod from 1959 to 1993. Crosses are at 10th  
581 percentile, mean and 90th percentile of variables.

582



583

584

585

586

587

588

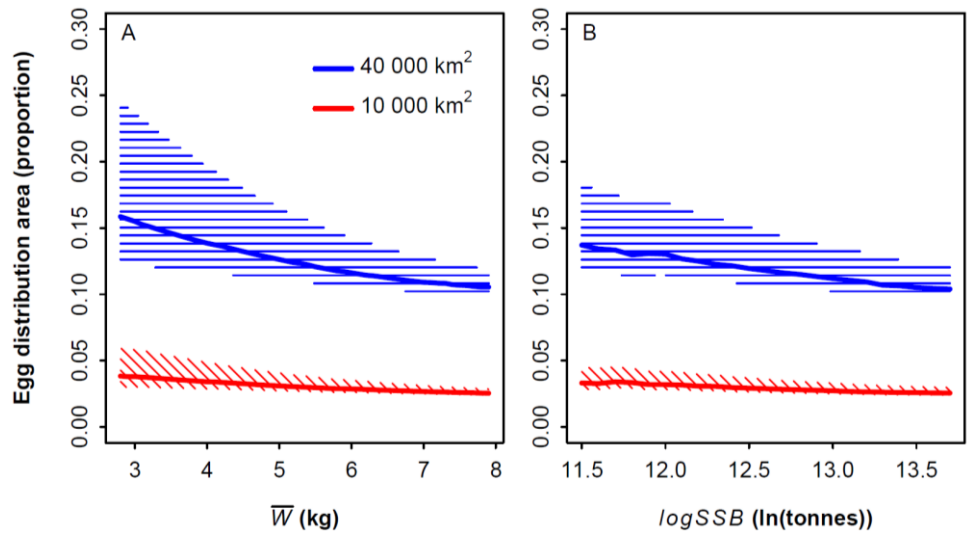
589

590

591

592

**Figure S2.** Simulated distribution of Northeast Arctic cod eggs at their locations halfway through the egg development. Red points in each panel represent eggs that experience oil concentrations above a threshold concentration of 0.1 ppb (left column) or 1.0 ppb (right column) at some point in their egg and larval life. Blue points (partly overlaid by the red points) represent remaining eggs. Upper and lower rows represent two different oil spill scenarios with filled yellow circles showing the release location.



593

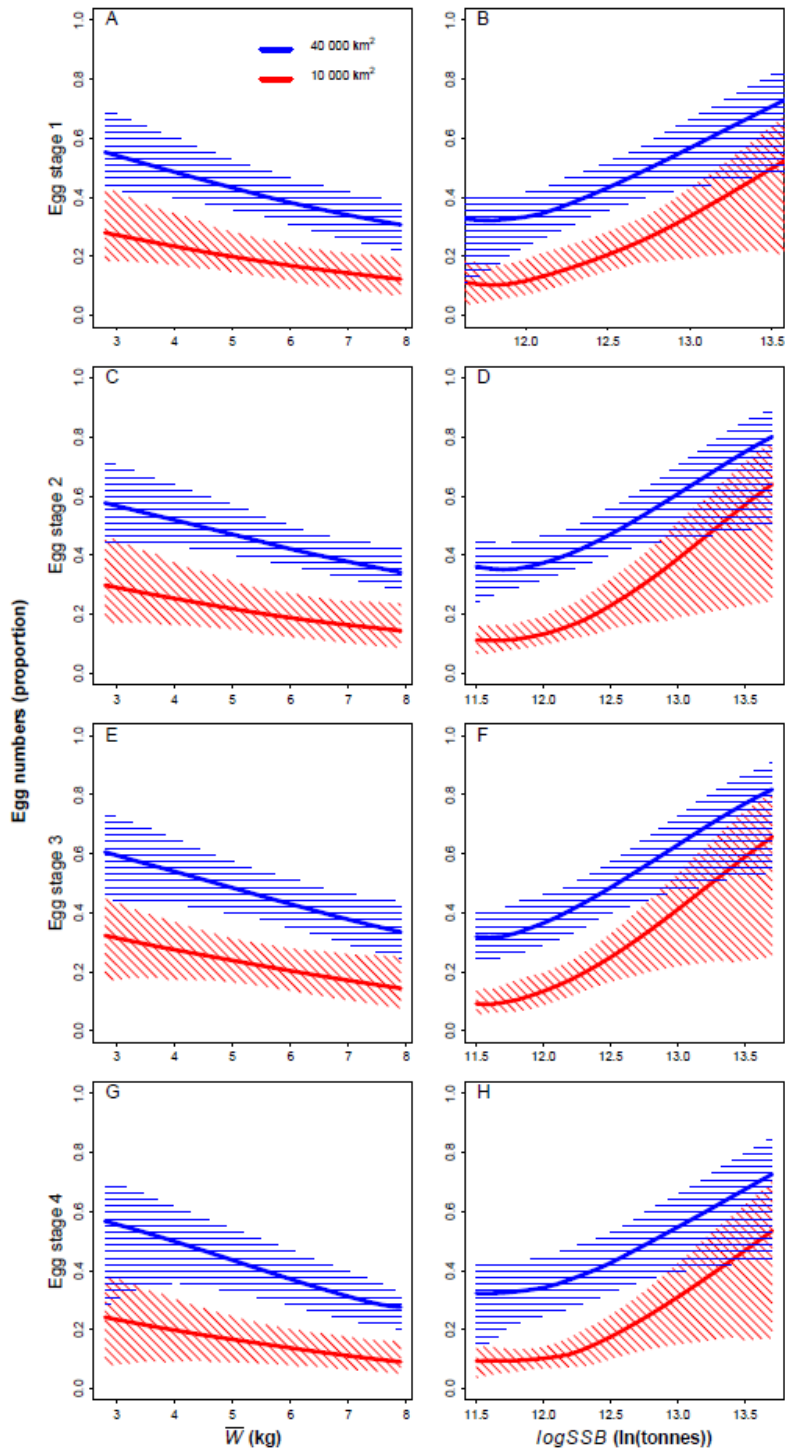
594

595

596

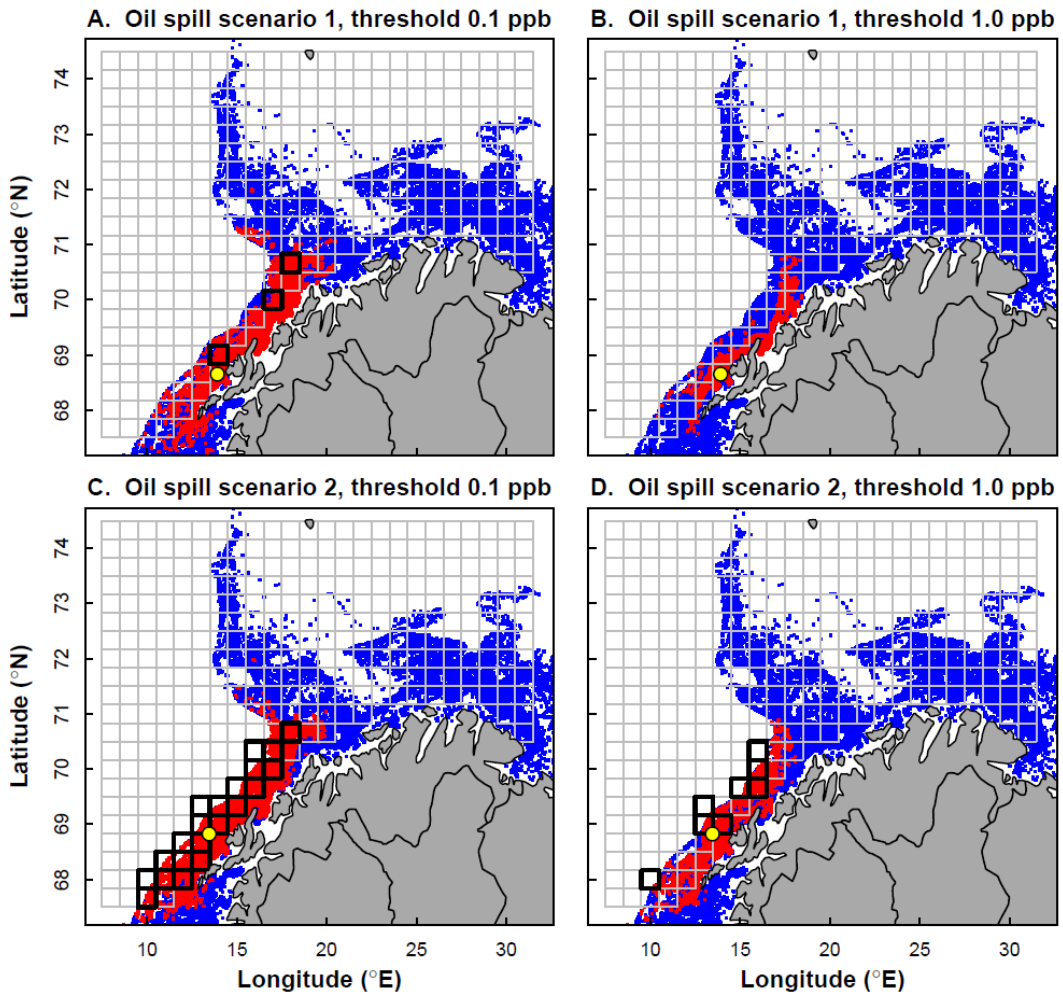
597

**Figure S3.** Maximal proportion of the total distribution area of Northeast Arctic cod eggs contained within areas of 10 000 km<sup>2</sup> or 40 000 km<sup>2</sup> dependent on (A)  $\bar{W}$  or (B) logSSB. Hatched lines represent 95 % confidence intervals.



598

599 **Figure S4.** Maximal proportion of Northeast Arctic cod eggs contained within  
600 areas of 10 000 km<sup>2</sup> or 40 000 km<sup>2</sup> dependent on (A, C, E, G) mean weight in  
601 the spawning stock,  $\bar{W}$ , or (B, D, F, H) spawning stock biomass,  $\logSSB$ . Each  
602 row shows results for one egg developmental stage. Hatched lines represent  
603 95 % confidence intervals (horizontal blue lines for 40 000 km<sup>2</sup>, oblique red  
604 lines for 10 000 km<sup>2</sup>).



605

606

607

608

609

610

611

612

613

614

615

**Figure S5.** Simulated distribution of Northeast Arctic cod eggs at their locations at 10<sup>th</sup> April 1997. Red points in each panel represent eggs that experience oil concentrations above a threshold concentration of 0.1 ppb (left column) or 1.0 ppb (right column) at some point in their egg and larval life. Blue points (partly overlaid by the red points) represent remaining eggs. Upper and lower rows represent two different oil spill scenarios with filled yellow circles showing the release location. Grey lines represent the grid used to predict egg distribution from the statistical model (**Fig. 1**). Grid cells with >50 % of particles experiencing above-threshold oil concentrations are shown in black.